Robust Adaptive and Repetitive Digital Tracking Control and Application to a Hydraulic Servo for Noncircular Machining

Tsu-Chin Tsao
Assistant Professor,
Department of Mechanical and Industrial Engineering,
University of Illinois at Urbana-Champaign,
Urbana, IL 61801

Masayoshi Tomizuka
Professor,
Department of Mechanical Engineering,
University of California, Berkeley, CA

This paper presents the development of robust digital tracking control algorithms and their real-time implementation on an electrohydraulic servo-actuator for tool positioning in noncircular machining. Robust adaptive feedforward controller for tracking arbitrary signals and robust repetitive controller for tracking periodic signals against disturbances and unmodeled dynamics have been developed. Experimental results are presented to illustrate the control system synthesis procedures and tracking performance.

1 Introduction

In tracking control problems, the control input must be applied so that the plant output follows a time varying desired output. This problem is closely related to system dynamic inverse. Intuitively speaking, if the dynamic inverse of a controlled plant is placed between the desired output signal and the control input, the plant output must come close to the desired signal. Of course, the problem is more complicated because of the stability and the realizability of inverse systems. When the problem duration is finite and the desired output signal is known in advance over the entire problem duration, the tracking problem can be formulated in an optimal control framework (Athans and Falb, 1966; Anderson and Moore, 1971). When the desired signal is not known over the entire problem duration but only locally, the tracking problem can be formulated as a finite preview problem (Tomizuka, 1975). The preview controller can be interpreted as a filter, which generates the optimal control input responding to previewed future desired outputs. Such filters can be designed in the frequency domain based on pole/zero cancellation and phase cancellation (Tomizuka, 1987). Design methods for tracking controllers mentioned above assume that the plant model is accurately known. When the controlled plant is poorly known and is subject to uncertainties and/or variations, the tracking controller must have adapting or learning capability so that an acceptable level of tracking performance is maintained.

A commonly used learning algorithm has the following integral form: $s_{k+1} = s_k + L_k e_k$, where k is a time index, s is a signal to be adjusted such that the error signal e converges to zero, and L is the learning gain. This integral form assures that the error converges to zero if the signal $s_{k+1} - s_k$ may converge to zero, but it requires special attention to the system stability. In this paper, we present two tracking control algorithms of this form, the robust adaptive feedforward tracking control algorithm and the robust repetitive control algorithm, for the tool motion generation in noncircular machining.

Noncircular machining generates a workpiece with noncircular shaped cross-sections by controlling the tool motion in the direction normal to the surface of the workpiece, for example, an oval shape engine piston. Tracking control algorithm for generating accurate dynamic tool motion is essential for successful implementation. This paper considers the use of an electrohydraulic servo actuator for tool motion generation.

The remainder of this paper is organized as follows. The next section presents a robust adaptive feedforward tracking control algorithm. Section 3 presents a robust repetitive control algorithm. Section 4 presents the implementation of the control algorithms on a hydraulic servo actuator for noncircular machining.

2 Robust Adaptive Feedforward Tracking Control Algorithm

The development of adaptive control has aimed at achieving both good robust stability and performance under plant dynamics uncertainties and variations. In tracking control, one approach is to use a fixed robust controller to stabilize the plant and to cascade the feedback system with an adaptive feed-forward controller to maintain specified tracking performance under plant variations. In this section, we are concerned with such approach.

Widrow and Stearn (1985) introduced the concept of adaptive inverse modeling and applied this concept to inverse control as well as signal processing techniques such as adaptive equalization, interference canceling, and beam forming. The effect of disturbances on the stability of the parameter estimation algorithms was analyzed from statistical considera-

Contributed by the Dynamic Systems and Control Division for publication in the JOURNAL OF DYNAMIC SYSTEMS, MEASUREMENT, AND CONTROL. Manuscript received by the DSCD January 18, 1989; revised manuscript received April 26, 1993. Associate Technical Editor: A. G. Ulsoy.

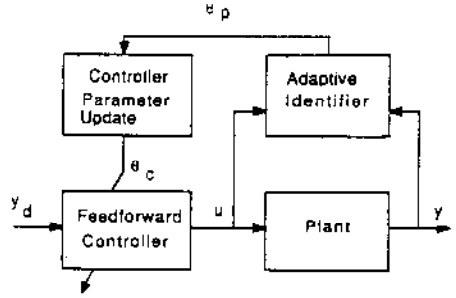

Fig. 1 Indirect adaptive feedforward tracking control system

tions. However, in various control applications, the available prior information about the disturbances is usually given, not in statistical terms, but as bounds on its absolute value. Thus, the probabilistic convergence arguments may be invalid (Lozano-Leal and Ortega, 1987). Tsao and Tomizuka (1987) gave a special type adaptive feed-forward control algorithm in which the convergence analysis was given in the deterministic sense without considering the effect of disturbances. In this paper, the problem of disturbances on the parameter estimation algorithms will be handled by utilizing the "relative dead zone" proposed by Kreisselmeier and Anderson (1986). Other methods such as projection of parameters to a constrained set (Goodwin and Sin, 1984) and estimator signal filtering will also be incorporated to achieve an integrated robust adaptive feedforward tracking system.

Figure 1 shows the block diagram of an indirect adaptive feed-forward control system. It consists of the plant to be controlled, the plant parameter estimation algorithm, the feedforward controller parameter adaptation algorithm and the calculation of the control input. The plant parameter estimation algorithm uses the plant input and output signals to generate the plant parameter estimates. The feed-forward controller adaptation algorithm takes the plant estimate as input and generates the controller parameters, which characterizes the plant inverse dynamics. Finally, the control input is calculated according to the obtained feed-forward controller.

While this procedure is described sequentially, the three parts described above can actually be executed asynchronously, i.e., the updating rates of the plant parameters, the controller parameters, and the control input can be different. For the convenience of presentation, we assume that the three updating rates are equal. The plant model, adaptive identifier, the feedforward controller, and performance characterization are described next.

The Plant Model. Suppose a SISO system has been stabilized and this stabilized closed-loop "plant" is described by a nominal discrete-time linear time invariant model:

$$A(q^{-1})y(k) = B(q^{-1})u(k-d) + \eta(k)$$

$$A(q^{-1}) = 1 + a_1 q^{-1} + a_2 q^{-2} + \ldots + a_n q^{-n}$$

$$B(q^{-1}) = b_0 + b_1 q^{-1} + \ldots + b_m q^{-m}, \quad (1)$$

where η includes those modeling error, disturbances and noises, q^{-1} is the one step delay shift operator, $A(q^{-1})$ and $B(q^{-1})$ are coprime and of degree n and m respectively, and $A(q^{-1})$ is monic and stable. The transfer function $q^{-d}B(q^{-1})/A(q^{-1})$ is called the tuned model of the actual system. The size of η can often be reduced by introducing an estimator filter $F(q^{-1})$ to u and y. Then Eq. (1) becomes

$$A(q^{-1})y_f(k) = B(q^{-1})u_f(k-d) + \eta_f(k) \quad (2)$$

or

$$y_f(k) = \theta^{*T}\phi(k-1) + \eta_f(k) \quad (3)$$

where $\eta_f(k) = F(q^{-1})\eta(k)$, $\theta^{*T} = [a_1, a_2, \ldots, a_n, b_0, b_1, \ldots, b_m]$, $\phi^T(k-1) = [-y_k(k-1), -y_f(k-2), \ldots, -y_f(k-n), u_f(k-d) \ldots, u_f(k-d-m)]$. Note that the tuned parameters θ^* is not required to be unique, especially when persistent excitation does not exist.

When η_f only contains small bounded disturbances and noises, a constant value N is sufficient to bound η_f. When η_f contains modeling error, it is relatively bounded (Kreisselmeier and Anderson, 1986) if there exist $\mu \geq 0$ and $m(0) \geq 0$ such that

$$\eta_f(k) \leq \mu m(k) \quad (4)$$

$$m(k) = \sigma_0 m(k-1) + |u_f(k-1)| + |y_f(k-1)| \quad (0 < \sigma_0 < 1) \quad (5)$$

In the case that the frequency contents of the input signal are concentrated at certain frequencies, the modeling error may be very small because the tuned model only fits the true plant at those frequencies. This is in contrast to the persistent excitation condition generally desirable for adaptive systems. In either case, it is assumed that the bound $N(k)$ is known apriori: i.e., $|\eta_f(k)| \leq N(k)$, $k > 0$.

Indirect Adaptive Feedforward Controller. The indirect adaptive feedforward controller consists of the adaptive identifier and the feedforward controller. The general form of an adaptive identifier is:

$$\theta(k) = \theta(k-1) + L(k)\phi(k-1)D(N(k), e_s(k)) \quad (6)$$

$$e_s(k) = y_f(k) - \theta^T(k-1)\phi(k-1), \quad (7)$$

where θ is the estimated parameter vector, e_s is the estimation error, L is the estimation gain matrix; $D(\ldots)$ is a "Relative Dead Zone" function to be precisely defined later. We postulate that the adaptive identifier has the following desirable properties for the purpose of synthesizing the adaptive feedforward controller:

(ID1) $$\|\theta(k)\| < \infty, \; k > 0, \quad (8)$$

(ID2) $$\frac{D^2(N(k), e_s(k))}{c + \phi^T(k-1)\phi(k-1)} \to 0 \text{ as } k \to \infty, \; (c < \infty) \quad (9)$$

(ID3) $$\theta(k) - \theta(k-1) \to 0 \text{ as } k \to \infty \quad (10)$$

Notice that only the convergence of the estimation error as in (ID2) is required and parameter convergence is not a concern except for the constraint in (ID1) and (ID3).

The control objective is to let the plant output $y(k)$ follow the signal $My_d(k + N_p)$, where M is the desired I/O map, y_d is the desired output signal and N_p is the preview length of y_d. This means that at time step k, the future reference points $y_d(k+1), \ldots, y_d(k+N_p)$ are known. To let y track y_d exactly, we may set $M(q^{-1}) = q^{-N_p}$.

Based on the estimated plant dynamics from the identifier, the (approximate) inverse dynamics can be obtained in several ways. Let the estimated plant transfer function at time k be $q^{-d}B_k(q^{-1})/A_k(q^{-1})$. Since the denominator $A_k(q^{-1})$ can be readily canceled, we assume the feed-forward controller is of the form

$$u(k) = (A_k W_k)(q^{-1})y_d(k+N_p), \quad (11)$$

The filter $W_k(q^{-1})$ is to be chosen to make the model following error $(M - q^{-d}B_k W_k)(q^{-1})$ small in some sense and is postulated to have the following properties:

(FF1)

$$W_k(q^{-1}) =: \frac{m_0(k) + m_1(k)q^{-1} + \ldots + m_l(k)q^{-l}}{1 + n_1(k)q^{-1} + \ldots + n_r(k)q^{-r}} \quad (12)$$

where the spectral radius of $W_k(q^{-1})$, denoted σ_k, satisfies

$$\sigma_k \leq 1 - \epsilon < 1 \text{ for } k > 0. \quad (13)$$

(FF2)

$$\|\theta_c(k)\| \leq c_1\|\theta(k)\| + c_2, \; k > 0, \quad (c1 > 0, \; c2 > 0) \quad (14)$$

where $\theta_c(k)$ is the parameter vector of the feedforward controller $(A_k W_k)(q^{-1})$.

Based on the construction of the above adaptive identifier and the feed-forward controller, the tracking performance can be characterized as follows:

Theorem 1: For the plant model of Eq. (3), the adaptive identifier satisfying (ID 1, 2, 3) and the feed-forward controller satisfying (FF1, 2), if the desired output y_d is uniformly bounded, then

$$\|\phi(k)\| < \infty \tag{15}$$

$$D(N(k), e_t(k)) \to 0 \text{ as } k \to \infty, \tag{16}$$

where

$$e_t(k) =: (FA_k)(q^{-1}) e_m(k),$$

$$e_m(k) =: (B_k W_k)(q^{-1}) y_d(k+N_p) - y(k). \tag{17}$$

Proof: See Appendix.

Remarks:

(1) This theorem gives a general result for the indirect adaptive feed-forward control system. It shows that the control input is uniformly bounded and $e_t(k)$ is relatively bounded by $N(k)$ asymptotically.

(2) The goal of tracking is to minimize the model following error $\{M(q^{-1}) y_d(k+N_p) - y(k)\}$. The adaptive feedforward controller should be designed such that $B_k W_k(q^{-1})$ is as close to $M(q^{-1})$ as possible. In the ideal situation, a small e_t implies that both e_m and the model following error are small. This situation does not hold when $A_k(q^{-1})$ is pathologic, i.e., when $A_k(q^{-1})$ contains roots on the unit circle asymptotically. In such situation, a small e_t may result from a persistent e_m filtered by $FA_k(q^{-1})$. The avoidance of pathologic $A_k(q^{-1})$ are discussed next.

(3) If the reference input is persistently exciting (Bai and Sastry, 1985), then the parameter estimates will converge to the neighborhood of the tuned model. Then, the pathology cannot happen since $A(q^{-1})$ is stable by assumption. However, the richness of the reference input is usually not assured.

(4) If $A_k(q^{-1}) \equiv 1$, i.e., the plant is modeled only by a FIR filter, then the problem with A_k does not exist. The tradeoff here is that a long FIR filter may be needed to achieve small modeling errors.

(5) Since the roots of $A(q^{-1})$ are inside the unit circle by assumption, we can constrain the parameter estimate $A_k(q^{-1})$ such that all its roots are in the unit circle at every time step. Such procedure is simple for lower order $A(q^{-1})$, yet is not easy if the order is larger than 3.

Parameter Estimation Algorithms. Since the plant model contains the error η_f, standard parameter estimation algorithms which do not consider the effect of η_f cannot be used. An idea is to turn off the estimator when the magnitude of the estimation error is reduced to the level of the modeling error η_f. The modified projection method and the least squares method, which apply the above idea, are given below.

Projection Method:

$$\theta(k) = \theta(k-1) + \frac{a\phi(k-1) D(N(k), e_s(k))}{c + \phi^T(k-1)\phi(k-1)} \quad (0<a<2,\ c>0) \tag{18}$$

$$D(N(k), e_s(k)) = \begin{cases} e_s(k) - N(k) & \text{if } e_s(k) > N(k) \\ 0 & \text{if } |e_s(k)| \le N(k) \\ e_s(k) + N(k) & \text{if } e_s(k) < -N(k) \end{cases} \tag{19}$$

Lemma 2 (Kreisselmeier and Anderson, 1986): Subject to the plant model Eq. (3) and $|\eta_f(k)| < N(k)$, the projection method described by Eqs. (18) and (19) has the properties (ID1-3).

Lemma 3 (Goodwin and Sin, 1984): If the dead zone function $D(N(k), e_s(k))$ in Eq. (19) is defined as:

$$D'(N(k), e_s(k)) = \begin{cases} e_s(k) & \text{if } |e_s(k)| > 2N(k) \\ 0 & \text{if } |e_s(k)| \le 2N(k) \end{cases} \tag{20}$$

and $0 < a < 1$. Then, (ID1), (ID3) are satisfied and (ID2) is replaced by

$$\frac{D'^2(N(k), e_s(k))}{c + \phi^T(k)\phi(k)} \to 0 \text{ as } k \to \infty. \tag{21}$$

In general, as much prior information of the plant as possible should be utilized for superior and robust performance. Two methods exist, one is based on constrained parameter estimation (Goodwin and Sin, 1984) and the other is based on model reparameterization (Bai and Sastry, 1986). For the purpose of our specific application presented later, we will only exploit the first method with the following type of linear constraints

$$\theta^T \nu_c \begin{cases} > \delta \text{ or} \\ = \delta \text{ or} \\ < \delta \end{cases} \tag{22}$$

where ν_c is a constraint vector and δ is a constant scalar.

When the parameter estimates in Eq. (18) do not satisfy the specified constraint, they are projected onto the constraint set by

$$\theta_p = \theta + \frac{(\delta - \theta^T \nu_c)\nu_c}{\nu_c^T \nu_c} \tag{23}$$

Then the projected parameter estimates are closer to the tuned parameters θ^* than the unprojected one.

Least Squares Method:

$$\theta(k) = \theta(k-1) + \frac{\lambda(k) P(k-1)\phi(k-1) e_s(k)}{1 + \lambda(k)\phi^T(k-1) P(k-1)\phi(k-1)} \tag{24}$$

$$P(k) = P(k-1) - \frac{\lambda(k) P(k-1)\phi(k-1)\phi^T(k-1) P(k-1)}{1 + \lambda(k)\phi^T(k-1) P(k-1)\phi(k-1)} \tag{25}$$

$$\lambda(k) = \begin{cases} \dfrac{\alpha}{1 + \phi^T(k-1) P(k-1)\phi(k-1)} \dfrac{D(\sqrt{1+\alpha} N(k), e_s(k))}{e_s(k)} & \text{if } e_s(k) \neq 0 \\ 0 \quad \text{if } e_s(k) = 0 \end{cases} \tag{26}$$

where $0 < \alpha < 1$ and D is as defined in Eq. (19).

Lemma 4 (Lozano-Leal and Ortega, 1987): Subject to the plant model Eq. (3) and $|\eta_f(k)| < N(k)$, the least squares algorithm described by Eqs. (24)-(26) satisfies (ID1) and (ID3) and (ID2) is replaced by

$$\frac{D^2(\sqrt{1+\alpha} N(k), e_s(k))}{c + \phi^T(k-1)\phi(k-1)} \to 0 \text{ as } k \to \infty. \tag{27}$$

Feed-Forward Controllers. The feed-forward controller consists of two parts. The first part is $A_k(q^{-1})$, which directly cancels the estimated plant poles. The second part is $W_k(q^{-1})$, whose spectral radius is less than one. $W_k(q^{-1})$ can be obtained in several ways independently of the adaptive identifier.

(1) Optimal Tracking: When $B_k(q^{-1})$ is invertible, we may simply let $W_k(q^{-1}) = M(q^{-1})/B_k(q^{-1})$. Unfortunately, this is usually not the case for sampled data systems (Astrom and Whittenmark, 1984). In the case that $B_k(q^{-1})$ is noninvertible,

optimal tracking can be defined as the infimum of the distance (using appropriate transfer function norm) between the reference model $M(q^{-1})$ and the achievable input/output map $B_k W_k(q^{-1})$, i.e.

$$J^{\text{opt}} = \text{infimum} \| M - B_k W_k \|. \tag{28}$$

(2) Inverse Modeling by a parallel identifier: Widrow and Stearns (1985) suggested to obtain the inverse model for $B_k(q^{-1})$ by running a parallel parameter estimation algorithm. In this process, the I/O signals are generated by

$$s_y(i) = B_k(q^{-1}) s_u(i), \tag{29}$$

where i is a recursion index. $B_k(q^{-1})$ cascaded with the inverse model $W_k(q^{-1})$ should be as close as possible to $M(q^{-1})$. Let $W_k(q^{-1})$ be a FIR filter, then

$$M(q^{-1}) s_u(i) = W_k(q^{-1}) s_y(i) + \mu(i) \tag{30}$$

where μ is the modeling error. The parameters of $W_k(q^{-1})$ can be obtained by running the estimation algorithm described previously. Since the input s_u is artificially generated, one can choose an input signal with its spectrum in the desirable range.

(3) Zero Phase Error Tracking: The previous two methods may require too much computation for real time implementation. Another method convenient for parameterization is the zero phase error tracking algorithm (Tomizuka, 1987). This algorithm cancels all the phase shift from $B_k(q^{-1})$ by letting

$$W_k(q^{-1}) = \frac{M(q^{-1}) B_k^*(q^{-1})}{b^2} \tag{31}$$

where $B_k^*(q^{-1}) = B_k(q)$ is a non-causal filter but the product $MB_k^*(q^{-1})$ should be a causal filter, and $b = B_k(1)$ for attaining an exact model matching at zero frequency. To be precise, Theorem 1 is applied to give the following corollary.

Corollary 5 (Adaptive Zero Phase Error Tracking): Consider the plant model Eq. (3) with apriori information: $B(1) \geq \delta_0 > 0$ (or $B(1) \leq -\delta_0 < 0$). Apply the feed-forward controller in Eq. (31) and the adaptive identifier Eq. (18) or (20) with the constrained parameter estimate Eq. (23) where $\nu_c^T = [0, 0, \ldots, 0; 1, 1, \ldots, 1]$ and $\delta = \delta_0$ ($\delta = -\delta_0$ for $B(1) \leq -\delta_0 < 0$). Then,

$$\| \phi(k) \| < \infty \tag{32}$$

$$D(N(k), e_t(k)) \to 0 \text{ as } k \to \infty, \tag{33}$$

where

$$e_t(k) = (FA_k)(q^{-1}) \left[y(k) - \frac{(MB_k B_k^*)(q^{-1})}{b^2} y_d(k) \right] \tag{34}$$

Proof: In order that (FF2) in Theorem 1 be satisfied, the sign of the plant static gain must be known apriori so that constrained parameter estimation may be applied to bound $B_k(1)$ away from zero. Consider the case of positive static gain: i.e.,

$$\frac{B(1)}{A(1)} > 0 \tag{35}$$

Since $A(q^{-1})$ is stable and monic by assumption, $A(1)$ must be a positive number; otherwise, if $A(1) < 0$, there exists a sufficiently large number β such that $A(\beta) > 0$, and a root exist in the interval $(1, \beta)$. Therefore, the above constraint is equivalent to

$$B(1) \geq \delta_0 > 0 \tag{36}$$

for some positive δ_0. This implies the constrained parameter estimation defined above. Similarly, if the static gain is negative, $B(1) \leq -\delta_0 < 0$. Thus, the Corollary holds by direct application of Theorem 1.

3 Robust Repetitive Control Algorithm

In noncircular machining, an important class of shapes, the cam-like shapes, is generated by periodic tool motion. Repetitive control achieves perfect tracking of periodic reference signal by applying internal model principle, assuming the period of the signal is known. The synthesis of repetitive control was first developed in the continuous time domain by Hara et al. (1988). A discrete time domain synthesis featuring fast error convergence and efficient computation was proposed by Tomizuka et al. (1989). Let the period of the reference signal be N_r and the repetitive controller for the plant model in Eq. (1) be:

$$\frac{u(k)}{e(k)} = \frac{R(q^{-1}) q^{-Nr}}{1 - q^{-Nr}} \tag{37}$$

By the internal model principle, the error due to periodic disturbances asymptotically converges to zero as long as the closed-loop system is stable. The prototype repetitive controller based on the idea of zero phase compensation (Tomizuka et al., 1989) is:

$$R(q^{-1}) = \frac{K_r A(q^{-1}) B^-(q)}{B^+(q^{-1}) b}, \quad 0 < K_r < 2,$$

$$b \geq \max |B^-(e^{-j\omega})|^2 \tag{38}$$

where $B(q^{-1}) = B^+(q^{-1}) B^-(q^{-1})$ and $B^-(q^{-1})$ contains all the unstable plant zeros. Infinitely large feedback gain at the repetitive signal frequencies is imposed to achieve perfect tracking.

In fact, it is impossible to construct an exponentially stabilizing continuous-time domain repetitive controller for strictly proper plants and a modified repetitive controller, which introduces a low-pass filter in the internal model, has been proposed to solve this problem (Hara et al., 1988). In the discrete-time domain, an exponentially stable repetitive control system can still be obtained without introducing the low-pass filter because only a finite number of frequencies are dealt with as opposed to an infinite number of frequencies in the continuous counterpart. However, high gain feedback inherently has poor robust stability and hence the modified repetitive controller with the low-pass filter should also be necessary for synthesizing robustly stable discrete system (Tsao, 1988). This can be manifested by considering the size of allowable additive perturbation to the nominal plant model G.

Lemma 6 (Astrom and Wittenmark, 1984). Define a perturbed plant $\tilde{G} \in A(G, r)$ if

$$|\tilde{G}(e^{-j\omega}) - G(e^{-j\omega})| < |r(\omega)| \text{ for } 0 \leq \omega \leq 2\pi, \tag{39}$$

and $\tilde{G}$ has the same number of unstable poles as G. Suppose the closed loop system of the nominal plant G with a feedback controller C is stable. Then the closed-loop system for every $\tilde{G} \in A(G, r)$ is stable if and only if

$$|r(\omega)| \leq \left| \frac{1 + G(e^{-j\omega}) C(e^{-j\omega})}{C(e^{-j\omega})} \right| \tag{40}$$

By this, the allowable additive plant perturbation for the prototype repetitive control system in Eq. (37) is

$$|r(\omega)| = \left| \frac{1 - (1 - G(e^{-j\omega}) R(e^{-j\omega})) e^{-jNr\omega}}{R(e^{-j\omega})} \right| \tag{41}$$

Notice that $|r(\omega)| = |G(e^{-j\omega})|$ for $\omega = i2\pi/N_r$, $i = 0, 1, 2, \ldots, N_r - 1$. This indicates that the allowable unmodeled dynamics $r(\omega)$ is small at the periodic modes at which infinitely high feedback gains are employed. Therefore, robust stability must be achieved by introducing a low-pass filter Q in the repetitive controller, similar to the modified repetitive controller for exponential stability in the continuous counterpart:

$$\frac{u(k)}{e(k)} = \frac{R(q^{-1}) Q(q^{-1}) q^{-Nr}}{1 - Q(q^{-1}) q^{-Nr}} \tag{42}$$

The introduction of the low-pass filter Q maintains the learning mechanism of the internal model at low frequencies while turns off the learning at high frequencies to retain robust

stability. The following theorem shows how the allowable additive plant perturbation is increased with respect to the low-pass filter Q.

Theorem 7. Suppose a repetitive controller in the form of Eq. (37), in which $R(q^{-1})$ is assumed stable, stabilizes the nominal plant $G(q^{-1})$. Let

$$Q(q^{-1}) = \frac{H(q^{-1})H(q)}{h^2}$$
$$h = \max |H(e^{-j\omega})| \tag{43}$$

under the constraint that $Q(q^{-1})R(q^{-1})q^{-Nr}$ is causal. Then

$$\frac{Q(q^{-1})R(q^{-1})q^{-Nr}}{1 - Q(q^{-1})q^{-Nr}} \tag{44}$$

also stabilizes $G(q^{-1})$. Furthermore, the allowable additive perturbation is

$$|r(\omega)| = \left| \frac{1 - Q(e^{-j\omega})(1 - G(e^{-j\omega})R(e^{-j\omega}))e^{-jNr\omega}}{Q(e^{-j\omega})R(e^{-j\omega})} \right| \tag{45}$$

Proof: The characteristic equation of the original stable control system is

$$1 + q^{-Nr}(G(q^{-1})R(q^{-1}) - 1) = 0 \tag{46}$$

and that of the modified repetitive control system is

$$1 + q^{-Nr}(G(q^{-1})R(q^{-1}) - 1)Q(q^{-1}) = 0 \tag{47}$$

Equation (46) can be considered as a unity feedback system with stable loop gain $z^{-Nr}(GR - 1)$. Hence by the Nyquist stability criterion its encirclement around the critical point (-1) is zero. For Eq. (47), the loop gain $z^{-Nr}(GR - 1)Q$ is also stable and also $0 \le Q(e^{-j\omega}) \le 1$. Therefore the number of encirclement remains zero, which implies the closed loop stability. Equation (45) is directly from application of Eq. (41). Q.E.D.

The allowable perturbation $r(\omega)$ at high frequencies becomes approximately $|1/RQ|$. For the robust prototype repetitive controller defined by Eqs. (38), (43), and (44), a simple criteria for synthesizing Q against unmodeled dynamics for robust stability is given below.

Corollary 8. The repetitive control system stabilized by Eqs. (38), (43), and (44) is robust stable for the perturbed plant $\tilde{G} \in A(G, G/Q)$

Proof: By Theorem 7, it is sufficient to show that

$$\left| \frac{G}{Q} \right| \le \left| \frac{1 - Qe^{-jNr\omega}(1 - RG)}{RQ} \right| \tag{48}$$

Noticing that $0 \le R(e^{-j\omega})G(e^{-j\omega}) \le 1$, and $0 \le Q(e^{-j\omega}) \le 1$, due to the zero phase characteristics, we have

$$\left| \frac{1 - Qe^{-jNr\omega}(1 - RG)}{RQ} \right| \ge \frac{|1 - |Q(1 - RG)||}{|RQ|} \tag{49}$$

$$= \frac{1 - Q(1 - RG)}{|RQ|} \ge \frac{1 - (1 - RG)}{|RQ|} = \left| \frac{G}{Q} \right| \tag{50}$$

Q.E.D.

This corollary gives an explicit relation between the filter Q and the unmodeled dynamics $|G - \tilde{G}|$, and hence is useful from practical design standpoint. One simply needs to choose Q such that its magnitude is less than that of $|G/G - \tilde{G}|$. Parallel development for multiplicative perturbation can be found in Tsao (1988).

4 Application to an Electrohydraulic Servo-Actuator for Noncircular Machining

Experimental System Description. Figure 2 shows the experimental system, which consists of a hydraulic linear actuator, an analog current amplifier, and a digital signal processor.

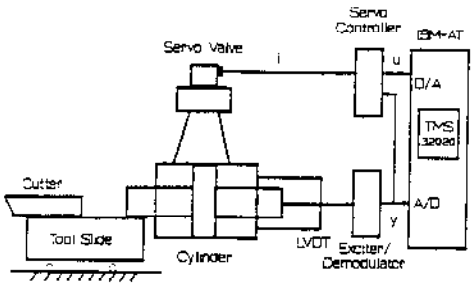

Fig. 2 Experimental system schematic diagram

The tool holder, which is a linear ball bearing sliding table, holds the cutting tool and is connected to the hydraulic actuator. The linear actuator is a double acting double rod cylinder with 50.8 mm stroke and 361.29 mm^2 effective area. Its front end is connected to the tool holder and its rear end is connected to a displacement sensor which is a linear variable differential transformer with a carrier frequency of 6000 Hz, implying approximately 600 Hz sensor bandwidth. The electrohydraulic servo valve is a two stage spring feedback flow control spool valve. The analog current amplifier sums up the negative feedback signal from the position sensor and the input from the computer digital to analog converter, and provides the current input to the servo valve torque motor. The dual-computer system consists of an IBM-AT microcomputer and a TMS-32020 digital signal processor. The TMS processor carries out the digital control and data acquisition by 32 bits integer arithmetic and 16 bits data word length. The IBM-AT, which can read and write data on the TMS memories, provides operator interface, and data storage for the TMS. The analog to digital converter has 5 micron per bit measurement resolution. Throughout the experiment the fluid supply pressure was 498.75 Pa (1500 psi) unless mentioned otherwise.

If we specify the cross-sectional shape of the workpiece by a series of points, the sampling period of the digital controller is determined by

$$T_s = \frac{1}{\frac{n_s}{60} N_p} \text{ second} \tag{51}$$

where n_s and N_p are the spindle speed in rpm and a required number of points to describe the cross-sectional shape, respectively. In this paper, $N_p = 250$ and $n_s = 600$ rpm, resulting in a sampling time of 0.4 ms. Every sampling was triggered by the pulse train signal from an encoder attached to the spindle axis.

System Identification. The system dynamics of hydraulic servo actuators are generally nonlinear and time varying. The nonlinearity is mainly due to the fact that the hydraulic fluid flow rate through an orifice is proportional to the square root of the pressure difference across the orifice. Coulomb friction and stiction between the piston rod and the sealing is another source of nonlinearity. The system variations are due to the effect of fluid temperature change, air trap in the system, mechanical wear and leakage, and etc.

The type-one open-loop hydraulic system was first stabilized by an analog proportional feedback controller. Figure 3 shows a set of step response data for several step sizes, normalized to unit step in the plot. Nonlinear effect can be clearly observed, a larger step caused larger overshoot. Small signal frequency response was obtained by the swept sine method and is shown in Fig. 4. The curve-fitted transfer function for this frequency response has a close agreement with the experimental result:

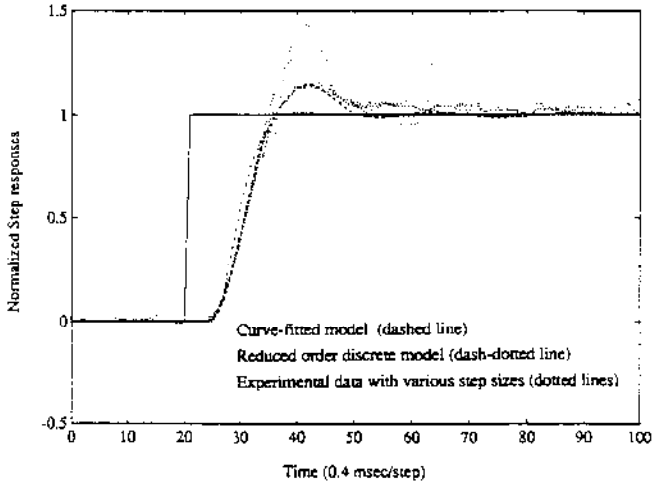

Fig. 3 Normalized step response plots

$$G(s)=\frac{1.21635e8\ \exp^{-7.5392e-4s}[(s+228.205)^2+701.581^2]}{[(s+293.720)^2+344.633^2][(s+136.264)^2+656.027^2]}\cdot\frac{[(s+383.750)^2+2052.592^2](s+2470)}{[(s+352.485)^2+1474.664^2][(s+350.602)^2+1801.829^2]} \quad (52)$$

The step response of this model shown in Figure 3 has a very close agreement with the experimental data with small step sizes. The zero-order-hold discrete transfer function for 0.4 msec. sampling time is

$$G(q)=\frac{1.45038e^{-3}(q+4.126)[(q-0.585)^2+0.628^2]}{q^2[(q-0.881)^2+0.122^2][(q-0.915)^2+0.246^2]}\cdot\frac{[(q-0.877)^2+0.253^2](q+0.319)(q-0.373)}{[(q-0.722)^2+0.483^2][(q-0.653)^2+0.574^2]}$$

or

$$G(q^{-1})=\frac{q^{-3}[0.00145+0.00167q^{-1}-0.01251q^{-2}+0.01884q^{-3}-0.01221q^{-4}+0.00217q^{-5}+0.00131q^{-6}-0.00044q^{-7}]}{1-6.34200q^{-1}+18.18757q^{-2}-30.81742q^{-3}+33.75890q^{-4}-24.49529q^{-5}+11.50632q^{-6}-3.20287q^{-7}+0.40505q^{-8}} \quad (53)$$

In order to test the effect of unmodeled dynamics on the performance of the developed robust tracking controllers, we signify the unmodeled dynamics by assuming that the discrete-time domain plant model is described by the following reduced order model

$$G(q^{-1})=\frac{q^{-d}(b_0+b_1q^{-1}+b_2q^{-2})}{1+a_1q^{-1}+a_2q^{-2}+a_3q^{-3}} \quad (54)$$

where d was determined to be 5 by inspecting the step responses and the parameters were obtained by off-line recursive least squares using random excitation:

$$(a_1, a_2, a_3, b_0, b_1, b_2) = (-0.606, -0.747, 0.519, 0.060, 0.034, 0.071) \quad (55)$$

Using the reduced order model for controller design also reduces the real-time implementation difficulty in computation. The frequency responses of both discrete models are shown in Fig. 4. The step response of the reduced order discrete model, shown in Fig. 3, has a good agreement with the experimental results in the rising stage but does not capture the overshoot as the full order model does.

Tracking control algorithms were tested by considering non-circular machining of a workpiece to an oval shape, shown in Fig. 5. Figure 5 also shows the experimental results of the zero

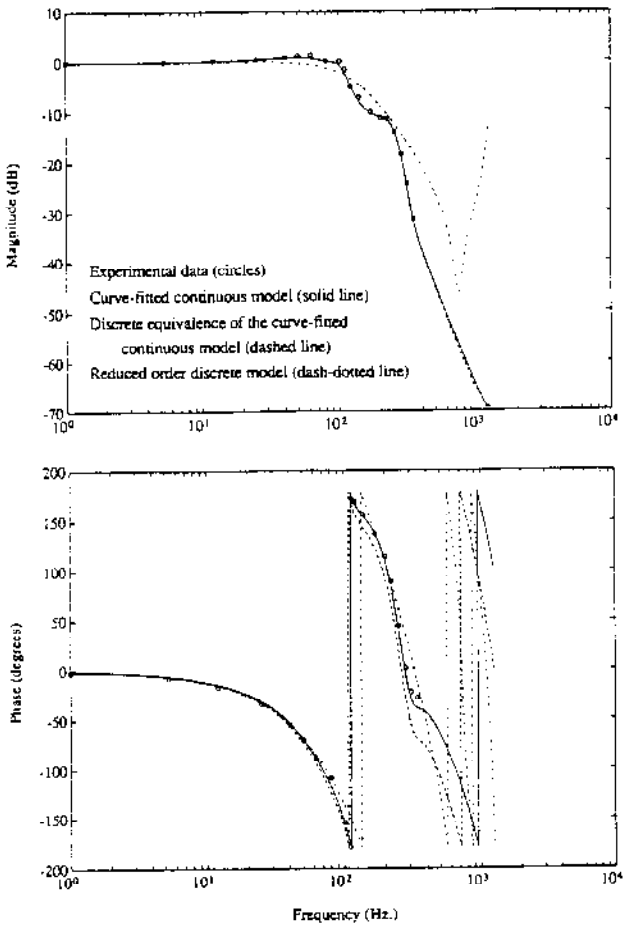

Fig. 4 Frequency response plots

phase error tracking controllers (ZPETC) based on the full order model in Eq. (53) and the reduced order model in Eq. (55), respectively. The control input for the full order model was computed off-line by floating point arithmetic. The control for the reduced order model was implemented in real time by 32 bits integer arithmetic with several scaling schemes to achieve appropriate dynamic range. The integer dynamic range was deemed appropriate when the results for the reduced order model using off-line floating point arithmetic made no significant difference from using real-time integer arithmetic. The ZPETC using the full order model rendered 4.5 units (5 microns/unit) r.m.s. tracking error compared to 9.7 units using the reduced order model.

Adaptive Zero Phase Error Tracking Controller. Adaptive zero phase error tracking control was tested among possible adaptive feedforward tracking control schemes because of its simplicity in implementation. The plant model structure assumed was the one in Eq. (54). Therefore the model parameters in Eq. (55) can be considered as one candidate of tuned models. This implies that adaptive ZPETC should be able to achieve a similar performance to that of tuned model.

The behavior of adaptive and repetitive controllers should be observed over a long time interval in order to conclude stability. Because of the limited memory space for storing the experimental data in real time, the data for the adaptive and repetitive controller experiments were collected and will be displayed in the following fashion: Each step in the horizontal axis represents one spindle revolution, which corresponds to 250 sampled data or 0.1 s of time interval. For each step, the

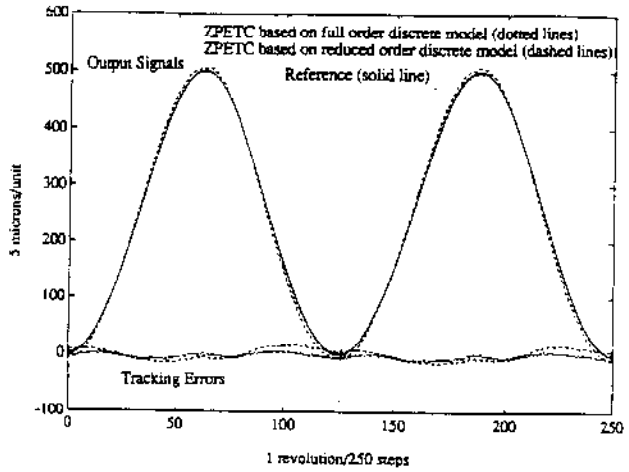

Fig. 5 Experimental results of ZPETC for an oval profile

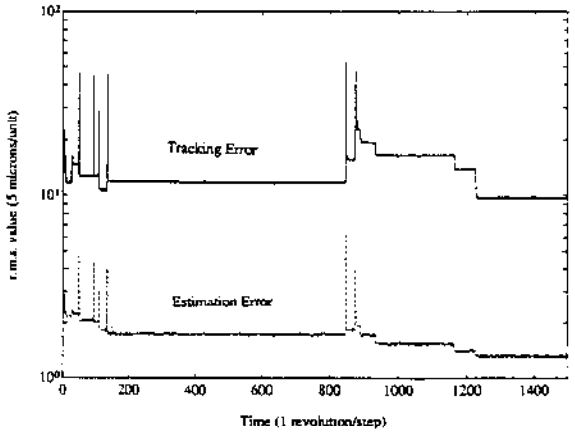

Fig. 6 Experimental results of adaptive ZPETC with insufficient dead zone size. $c = 10$, $F = (1 + q^{-1} + q^{-2} + q^{-3})/4$, $N = 2$, $a = 1.0$.

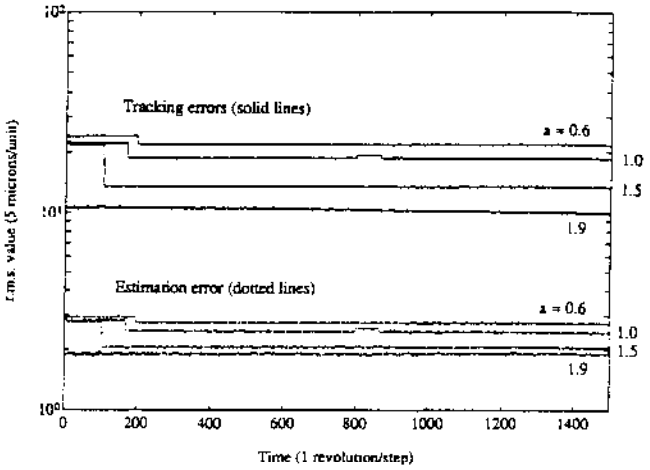

Fig. 7 Experimental results of adaptive ZPETC with adequate dead zone size. $c = 10$, $F = (1 + q^{-1} + q^{-2} + q^{-3})/4$, $N = 3$, $a = 0.6, 1.0, 1.5, 1.9$

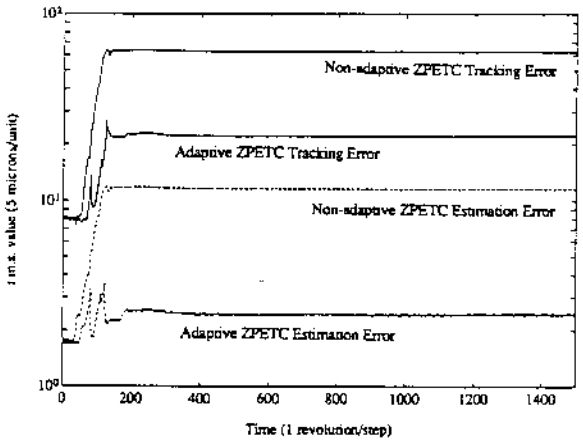

Fig. 8 Responses of adaptive and nonadaptive ZPETC when supply pressure was suddenly changed

r.m.s. values of signals over one spindle rotation are shown in the vertical axis.

Because the stabilized servo actuator has unity d.c. gain due to the fact that the actuator is of type-one in open loop, this prior information was utilized to constrain the estimated parameters by projection, as in Eqs. (22) and (36):

Constraints: $\theta^T \nu_c = 1$, where $\nu_c^T = (-1, -1, -1; 1, 1, 1)$,

and

$$\theta^T \nu_c > 0.001, \text{ where } \nu_c^T = (0, 0, 0; 1, 1, 1). \quad (56)$$

Because of the presence of noise and unmodeled dynamics, signal filtering and dead zone was necessary to ensure parameter estimate convergence. The noise level in the displacement measurement was about two to three units (A/D bits). An extensive set of experiments indicated that a moving average filter given below and a dead zone size of 3 were adequate. Figures 6 and 7 show the experimental results of adaptive ZPETC using projection scheme in Eq. (18) and dead zone function Eq. (20) with the following parameters and filters:

Figure 6: $c = 10$, $F(q^{-1})$

$$= (1 + q^{-1} + q^{-2} + q^{-3})/4, \; N = 2, \; a = 1.0,$$

Figure 7: $c = 10$, $F(q^{-1}) = (1 + q^{-1} + q^{-2} + q^{-3})/4$, $N = 3$,

$$a = 0.6, \; 1.0, \; 1.5, \; 1.9, \; 2.0.$$

Notice that in Fig. 6, the case of dead zone size $N = 2$, bursts appeared in the tracking error and the adaptive identifier estimation error e_s (per Eq. (7)). This is in contrast to the case of adequate dead zone $N = 3$ in Fig. 7.

Larger adaptation gains rendered smaller estimation and tracking errors until instability occurred at $a = 2.0$. This is compared to the condition in Lemma 3, in which $0 < a < 1$ is sufficient for convergence. The tracking error for the case $a = 1.9$ has reached 9.5 units (r.m.s.) similar to that attained by using the "tuned reduced order model."

To further illustrate the adaptive control capability, another experiment was conducted to investigate the effect of plant parameter and structure variations to tracking performance. The hydraulic supply pressure was suddenly reduced to 83.125 Pa (250 psi.) from 498.75 Pa (1500 psi) in the experiment to cause such change. The non-adaptive and the adaptive ZPETC (with $a = 1.5$) were tested. Figure 8 shows that the nonadaptive ZPETC could not properly compensate for the plant dynamics change and resulted in a significantly larger tracking error and estimation error than those of adaptive case. In the adaptive case, the estimation error for the lower supply pressure could not recover to the level of the higher supply pressure because the system dynamics had changed drastically from the assumed plant model structure.

Robust Repetitive Controller. The repetitive controller was designed based on the reduced order model in Eq. (55). The compensator $R(q^{-1})$ in the repetitive controller is simply the ZPETC:

$$R(q^{-1}) = \frac{q^5(1 - 0.606q^{-1} - 0.747q^{-2})(0.060 + 0.034q + 0.071q^2)}{(0.060 + 0.034 + 0.071)^2} \quad (57)$$

Since significant unmodeled dynamics exist, the closed loop

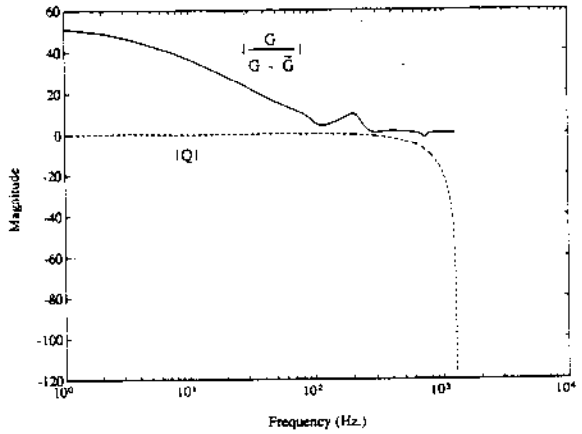

Fig. 9 Robust stability established with $Q = (1 + q^{-1})(1 + q)/4$

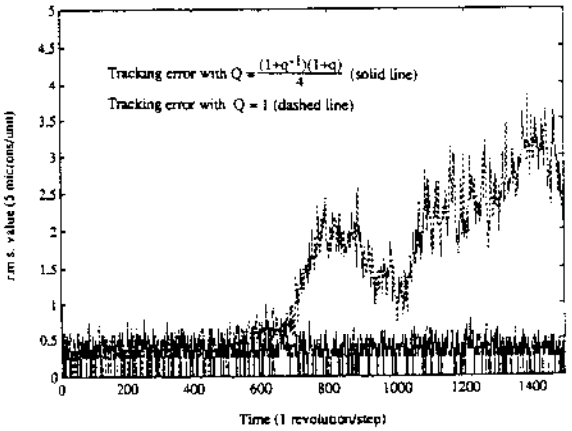

Fig. 10 Experimental results of repetitive control—effect of the Q filter

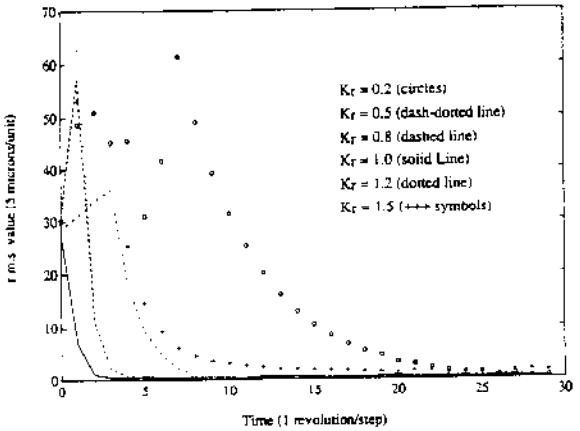

Fig. 11 Error convergence rates of repetitive control—effect of K_r

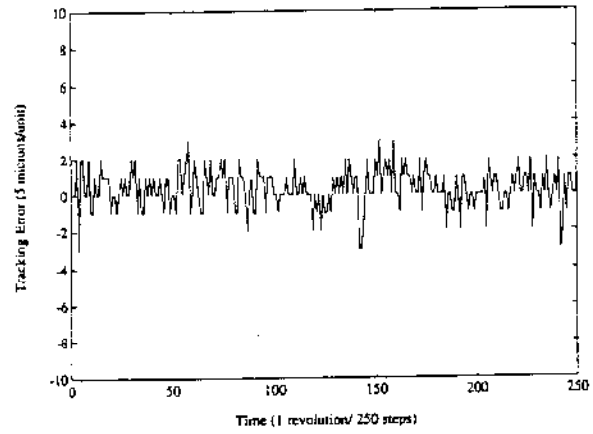

Fig. 12 A sample of steady state repetitive control tracking errors

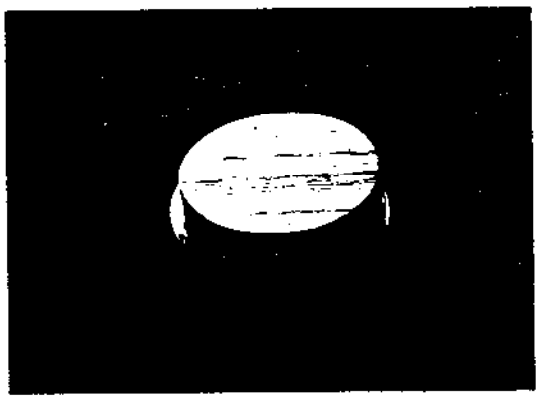

Fig. 13 A sample of machined workpiece

stability could not be established simply by employing $R(q^{-1})$. In this case, $Q(q^{-1})$ is chosen to achieve (robust) stability at the expense of reduced tracking accuracy. Corollary 8 was used to determine $Q(q^{-1})$ by using the form

$$Q(q^{-1}) = \left[\frac{(1+q^{-1})(1+q)}{4}\right]^n \tag{58}$$

Herein, the nominal plant G is the reduced order model in Eq. (55) and the perturbed plant \o($\tilde{G}$) is the curve-fitted full order model in Eq. (53). The magnitudes of Q and $\frac{G}{r}$ ($r = G - \tilde{G}$) shown in Fig. 9 indicate that the order $n = 1$ is sufficient to stabilize the perturbed plant, while $n = 0$ (i.e., $Q(q^{-1}) = 1$) violates the robust stability condition due to the small dip of G/r below 0 dB at around 700 Hz. The experimental results for both $n = 0$ and $n = 1$ with $Kr = 1.0$ are shown in Fig. 10. Notice that the evolution to instability for the case $Q(q^{-1}) = 1$ is not evident until after 600 revolutions.

The error convergence rate for the repetitive controllers is determined by the accuracy of the model as well as by the repetitive control gain K_r. For a reasonably accurate plant model $K_r = 1$ gives fastest convergence rate and even gives a dead beat controller for a perfectly modeled minimum phase plant (Tomizuka et al., 1989). The transient behaviors of the tracking error r.m.s. values under different repetitive control gains k_r are shown in Fig. 11. As expected, $k_r = 1.0$ had the fastest convergent rate. A sample of typical steady state tracking error signal, which is almost vanished except for noises, is shown over one revolution in Fig. 12.

Actual machining of Aluminum (7075-T651) was conducted using the robust repetitive controller because of its superior performance in tracking periodic reference signals. The radial cutting force was much smaller than the hydraulic actuator force capability and did not affect the tracking performance significantly. A sample of the machined oval workpieces is shown in Fig. 13.

5 Conclusions

Robust adaptive feedforward tracking controller and robust repetitive controller has been developed for tracking arbitrary dynamic signals and repetitive signals, respectively. Because both algorithms involve integration type of learning, establishing stability was the key factor for successful implementation. Application to a hydraulic servo system shows that robust parameter estimation by a combination of signal filtering, dead zone, and parameter constraints is crucial for successful adaptive tracking control implementation. For repetitive control, a low-pass filter, which turns off high gain feedback learning at high frequencies, is crucial for establishing system stability. This low-pass filter has been explicitly related to unmodeled dynamics for convenience in practical design.

Acknowledgment

This work was supported in part by National Science Foundation through grant No. DMC-8508412.

References

Astrom, K., and Whittenmark, 1984, *Computer Controlled Systems*, Prentice Hall, Englewood Cliffs, N.J.

Anderson, B. D. O., and Moore, J. B., 1971, *Linear Optimal Control*, Prentice Hall, Englewood Cliffs, N.J.

Athans, M., and Falb, P., 1966, *Optimal Control*, McGraw-Hill Book Company.

Bai, E. W., and Sastry, S. S., 1986, "Discrete Time Adaptive Control Utilizing Prior Information" *IEEE Trans. on Automatic Control*, Vol. 31, No. 8, pp. 779–782.

Goodwin, G. C., and Sin, K. S., 1984, *Adaptive Filtering Prediction And Control*, Prentice Hall, Englewood Cliffs, N.J.

Goodwin, G. C., Lozano-Leal, R., Mayne, D. Q., and Middleton, R. H., 1986, "Reapprochement between Continuous and Discrete Model Reference Adaptive Control" *Automatica*, Vol. 2, No. 2, pp. 199–207.

Hara, S., Yamamoto, Y., Omata, T., and Nakano, M., 1988, "Repetitive Control System: A New Type Servo System for Periodic Exogenous Signals," *IEEE Trans. Automatic Control*, Vol. 33, No. 7, pp. 659–668.

Kreisselmeier, Gerhard, and Anderson, B. D. O., 1986, "Robust Model Reference Adaptive Control" *IEEE Trans. Automatic Control*, Vol. AC-31, No. 2, pp. 127–133.

Lozano-Leal, R., and Ortega, R., 1987, "Reformulation of the Parameter Identification Problem for Systems with Bounded Disturbances," *Automatica*, Vol. 23, No. 2, pp. 247–251.

Tomizuka, M., and Whitney, D. E., 1975, "Optimal Discrete Finite Preview Problem (Why and How is Future Information Important?)," ASME JOURNAL OF DYNAMIC SYSTEMS, MEASUREMENT, AND CONTROL, Vol. 97, No. 4, pp. 319–325.

Tomizuka, M., 1987, "Zero Phase Error Tracking Algorithm for Digital Control," ASME JOURNAL OF DYNAMIC SYSTEMS, MEASUREMENT, AND CONTROL, Vol. 109, No. 1, pp. 65–68.

Tomizuka, M., Tsao, T.-C., and Chew, K., 1989, "Analysis and Synthesis of Discrete-Time Repetitive Controllers," ASME JOURNAL OF DYNAMIC SYSTEMS, MEASUREMENT, AND CONTROL, Vol. 111, pp. 353–358.

Tsao, T. C., and Tomizuka, M., 1987, "Adaptive Zero Phase Error Tracking Algorithm for Digital Control," ASME JOURNAL OF DYNAMIC SYSTEMS, MEASUREMENT, AND CONTROL, Vol. 109, pp. 349–354.

Tsao, T-C., and Tomizuka, M., 1988, "Adaptive and Repetitive Digital Control Algorithms for Noncircular Machining," *Proc. American Control Conference*, Atlanta, GA, pp. 115–120.

Tsao, T-C., 1988, "Digital Tracking Control and Its Application to Noncircular Machining," Ph.D. dissertation, Univ. of California—Berkeley.

Widrow, B., and Stearns, S. D., 1985, *Adaptive Signal Processing*, Prentice Hall, Englewood Cliffs, N.J.

APPENDIX

Proof of Theorem 1

We first show the boundness of $\phi(k)$ using the Lemma following this proof. Consider the state representation of W_k. The conditions in Eqs. (A6), (A7), and (A8) for the Lemma are satisfied by (ID1), (FF1), and (ID3), respectively. Therefore, (A9) applies. Since the state of a linear system cannot grow unbounded in finite time, $\|x(n_0)\| < \infty$. Therefore, $\|\phi(k)\| < \infty$ in view of Eq. (A9). By (ID2), it follows that

$$D(N(k), e_s(k)) = 0 - 0 \text{ as } k \to \infty. \tag{A1}$$

Notice that the following two time varying operations are different (Goodwin and Sin, 1984), i.e.,

$$(A_k B_k)(q^{-1})w(k) = \sum_i \sum_j a_i(k) b_j(k) w(k-i-j)$$

$$= (B_k A_k)(q^{-1})w(k) \tag{A2}$$

$$A_k(q^{-1}) \cdot B_k(q^{-1})w(k) = \sum_i \sum_j a_i(k) b_j(k-i) w(k-i-j)$$

$$\neq B_k(q^{-1}) \cdot A_k(q^{-1})w(k) \tag{A3}$$

First equation means that $w(k)$ is operated on the product of A_k and B_k. The second equation means that $w(k)$ is first operated on B_k and then A_k. However, if $w(k)$ is uniformly bounded and $A_k - A_{k-1}$, $B_k - B_{k-1}$ converges to zero asymptotically, $A_k \cdot B_k w(k)$, $B_k \cdot A_k w(k)$ and $(A_k B_k)w(k)$ are indistinguishable asymptotically. Therefore, $e(k)$ and $e_t(k)$ are asymptotically identical as shown below.

$$\lim_{k\to\infty} e_s(k) - e_t(k) = \lim_{k\to\infty} [A_{k-1} y_f(k) - B_{k-1} u_f(k)]$$

$$- F A_k [y(k) - B_k W_k y_d(k + N_p)]$$

$$= \lim_{k\to\infty} A_{k-1} \cdot F y(k) - A_k F y(k) - B_{k-1} \cdot F u(k) + B_k F u(k)$$

$$- (B_k F) \cdot [(W_k A_k) y_d(k + N_p)] - (F A_k) \cdot [(B_k W_k) y_d(k + N_p)]$$

$$= 0 \tag{A4}$$

where (ID1), (ID3), and boundness of $y(k)$, $u(k)$, $W_k y_d(k + N_p)$ have been utilized. Equation (16) then follows from Eqs. (A1) and (A4).

Lemma (Goodwin, et al., 1986): Consider the system:

$$x(k+1) = A(k)x(k) + B(k)u(k)$$

$$y(k) = C(k)x(k) + D(k)u(k) \tag{A5}$$

Then provided

(i) $\|A(k)\|$, $\|B(k)\|$, $\|C(k)\|$, $\|D(k)\|$ are bounded for all k, (A6)

(ii) Spectral radius of $A(k) \leq 1 - \epsilon < 1$ for all $k \geq n_0$, and (A7)

(iii) $\sup_{k \geq n_0} \|A(k+1) - A(k)\|$ is sufficiently small, (A8)

the system, Eq. (A5), is BIBO stable in the sense that there exist $0 \leq m_1 < \infty$, $0 \leq m_2 < \infty$, which are independent of k and n_0 such that

$$|y(N)| \leq m_1 \|x(n_0)\| + m_2 u_{\max} \tag{A9}$$

$u_{\max} = \max_{n_0 \leq \tau \leq N} |u(\tau)|$ for all $N \geq k \geq n_0$.